Contribution from the Departments of Chemistry, North Carolina State University, Raleigh, North Carolina 27695, and The University of North Carolina at Charlotte, Charlotte, North Carolina 28223, and Naval Research Laboratory, Washington, D.C. 20375

Surface-Modified Electrodes: Oxidative Electropolymerization and Deposition of Ni[Me_4($RBzo)_2$[14]tetraeneN_4] Complexes[1]

Cynthia L. Bailey,[†] Robert D. Bereman,*[†] D. Paul Rillema,*[‡] and Robert Nowak[§]

Received June 27, 1985

A series of surface-modified electrodes based on the oxidative electropolymerization of the monomeric complexes Ni[Me_4-($RBzo)_2$[14]tetraeneN_4] (R = CH_3, H, Cl, CO_2CH_3, $CO_2C_3H_7$, and NO_2) were examined. The monomers polymerize to give polymers of the form [Ni(Me_4($RBzo)_4$[14]tetraeneN_4)]$_n$, which form thin films on electrode surfaces. These films form on the electrode by constant-potential electrolysis at 1.4 V, cycling from +1.4 to −2.0 V, and cycling from 0 to 1.4 V vs. SSCE. Films form on Pt, Au, glassy-carbon, and SnO_2 surfaces in acetonitrile, methylene chloride, and propylene carbonate solutions containing various tetraalkylammonium salts as electrolytes. The magnitude of film growth depends on the method of deposition, the solvent, and the rate of cycling; i.e., five cycles from +1.4 to −2.0 V vs. SSCE (at a scanning rate of 200 mV/s) resulted in 124 "monolayers" forming on a Pt disk electrode in an acetonitrile solution, which was 0.1 M in TEAP and gave 185 "monolayers" at 50 mV/s and 12 "monolayers" in propylene carbonate at 200 mV/s. Film growth was also dependent on the electrolyte and the electrode surface. The modified electrodes, when transferred to neat electrolyte solutions, continued to exhibit three surface waves. For various R derivatives, $E_0'(1)$ ranged from 0.51 to 0.70 V, $E_0'(2)$ ranged from 0.92 to 1.12 V, and $E_0'(3)$ ranged from −1.25 to −1.84 V vs. SSCE. $E_0'(1)$ and $E_0'(2)$ were assigned as ligand oxidations; $E_0'(3)$ was assigned as a metal-centered reduction. The surface of the film appeared smooth; however, at higher SEM magnification the surface exhibited a ridged appearance. Visible and infrared spectra suggest that the nickel macrocycle remained in the film; XPS data indicated that the Ni to N ratio was 1:4.

Introduction

Tetraazaannulene macrocyclic ligands have served as models for such naturally occurring systems as porphyrins and corrin rings, which are found in heme proteins, chlorophylls, and metalloenzymes. Consequently, a large number of derivatives containing various metals such as Co(II),[2] Cu(II),[3] Fe(II),[4] Mn(III),[5] Ni(II),[6] Re(I),[7] Rh(I),[7] Pd(II),[8a] Ru(II),[8b] and $V^{IV}O$[9] have been synthesized with hopes that some would mimic biological functions. Indeed, several complexes have been effective as catalysts in the solid state. In particular, cobalt tetraazaannulene has been exploited as a dioxygen reduction catalyst at cathodes in fuel cells[10] and a nickel tetraazaannulene surface-modified electrode was used to catalyze the oxidation of water.[11] In general, the electrodes were modified by thermal treatment after the solid tetraazaannulene was deposited by evaporation techniques on the electrode surface.[12] Other techniques such as oxidative deposition,[11] reductive deposition,[13] and slurries[14] have also been used to yield modified electrodes.

Recently, we reported the preparation and properties of a series of nickel complexes containing the tetraazaannulene ligand [Me_4($RBzo)_2$[14]tetraeneN_4]$^{2-}$ where R was CH_3, H, Cl, CO_2-CH_3, $CO_2(CH_2)_2CH_3$, and NO_2 (Figure 1).[15] Cyclic voltammograms of these complexes exhibited two irreversible oxidations that ranged from 0.39 to 0.82 V and from 0.9 to 1.34 V and a reversible reduction in the −1.5 to −1.8 V range vs. SSCE. Upon repetitive scanning in the oxidative region, we found films grew reproducibly on the electrode surface and remained electroactive. Subsequently we have found that other metallotetraazaannulenes exhibit the same property. The film appears to form by direct linkage of the macrocycles by bond formation involving the δ carbon atom of the ligand's diiminate backbone in a manner similar to that found in formation of binuclear complexes reported by Dabrowiak et al.[16]

This is the first in a series of papers that will systematically investigate the nature and properties of these films. The films are intriguing to us from several viewpoints. Surface-modified electrodes can potentially mimic the catalytic redox behavior of biological systems. In addition, these surface-modified electrodes should also facilitate CO_2 reduction since similar Ni(II) monomer complexes are known to bind CO_2.[17]

Experimental Section

Materials. Tetraalkylammonium salts were purchased from Southwestern Analytical Chemicals, Inc., dried overnight at 70 °C under vacuum, and used without further purification. Aldrich Gold Label acetonitrile, Fisher Spectranalyzed methylene chloride, and Burdick and Jackson "distilled in glass" propylene carbonate were dried 48 h over 4 Å molecular sieves before use. All other solvents were reagent grade and used without further purification. Argon was scrubbed by passing it through a 2 M solution of perchloric acid and a 0.2 M solution of chromous perchlorate generated from chromic perchlorate over zinc amalgam.

The preparation and solution redox chemistry of the nickel tetraazaannulene complexes were described previously.[15]

Physical Measurements. Electronic absorption spectra were obtained in *N,N'*-dimethylformamide (DMF) solutions using matched 1-cm quartz cells and were recorded with a Cary 14 recording spectrophotometer. Transmission spectra were recorded by using SnO_2 or quartz plates and were recorded on a Cary 14 recording spectrophotometer.

Infrared spectra were recorded over the range 4000–500 cm^{-1} on a Perkin-Elmer Model 521 spectrometer and a Nicolet 20DX FT IR as KBr pellets or Nujol mulls. Scanning electron micrographs were obtained with a JEOL JSM-35CF scanning electron microscope at 20 keV.

[†] North Carolina State University.
[‡] The University of North Carolina at Charlotte.
[§] Naval Research Laboratory.

(1) A preliminary account of this work was given at the 188th National Meeting of the American Chemical Society, Philadelphia, PA, Aug 1984.
(2) (a) Jager, E. G. *Z. Anorg. Allg. Chem.* **1969**, *364*, 177. (b) Weiss, M. C.; Goedken, V. L. *J. Am. Chem. Soc.* **1976**, *98*, 3389. (c) Weiss, M. C.; Gordon, G. C.; Goedken, V. L. *J. Am. Chem. Soc.* **1979**, *101*, 857.
(3) L'Eplanttender, F. A.; Pugin, A. *Helv. Chem. Acta* **1975**, *58*, 917.
(4) (a) Truex, T. J.; Holm, R. H. *J. Am. Chem. Soc.* **1971**, *93*, 285. (b) Goedkin, V. L.; Pluth, J. J.; Ping, S.-M.; Bursten, B. *J. Am. Chem. Soc.* **1976**, *98*, 8014.
(5) Sakata, K.; Nakanura, H.; Hashimoto, M. *Inorg. Chim. Acta* **1984**, *83*, L67.
(6) (a) Place, D. A.; Ferrara, G. P.; Harland, J. J.; Dabrowiak, J. C. *J. Heterocycl. Chem.* **1980**, *17*, 439. (b) Ferrara, G. P.; Dabrowiak, J. C. *Inorg. Nucl. Chem. Lett.* **1978**, *14*, 31. (c) Hanke, R.; Breitmaier, E. *Chem. Ber.* **1982**, *115*, 1657.
(7) Kadish, K. M.; Bottomley, L. A.; Schaeper, B.; Tsutsui, M.; Bobsein, R. L. *Inorg. Chim. Acta* **1979**, *36*, 219.
(8) (a) Tsutsui, M.; Bobsein, R. L.; Cash, G.; Pettersen, R. *Inorg. Chem.* **1979**, *18*, 758. (b) Warren, L. F.; Goedkin, V. L. *J. Chem. Soc., Chem. Commun.* **1978**, 909.
(9) (a) Sakata, K.; Hashumoto, M.; Tagani, N.; Morakumi, Y. *Bull. Chem. Soc. Jpn.* **1980**, *53*, 2262. (b) Goedken, V. L.; Ladd, J. A. *J. Chem. Soc., Chem. Commun.* **1981**, 910.
(10) Clauberg, B. W.; Sandstede, G. *J. Electroanal. Chem. Interfacial Electrochem.* **1976**, *74*, 393.
(11) Issahary, D. A.; Ginzburg, G.; Polak, M.; Meyerstein, B. *J. Chem. Soc., Chem. Commun.* **1982**, 441.
(12) Gruenig, G.; Weisener, K.; Gamburzev, S. Iliev, I.; Kaisheva, A. *J. Electroanal. Chem. Interfacial Electrochem.* **1983**, *159*, 155.
(13) Yamana, M.; Darby, R.; Dhar, H. P.; White, R. E. *J. Electroanal. Chem. Interfacial Electrochem.* **1983**, *152*, 261.
(14) Beck, F. *J. Electroanal. Chem. Interfacial Electrochem.* **1977**, *81*, 197.
(15) Bailey, C. L.; Bereman, R. D.; Rillema, D. P.; Nowak, R. *Inorg. Chem.* **1984**, *23*, 3956.
(16) McElroy, F. C.; Dabrowiak, J. C. *J. Am. Chem. Soc.* **1976**, *98*, 7112.
(17) Fisher, B.; Eisenberg, R. *J. Am. Chem. Soc.* **1980**, *102*, 7361.

0020-1669/86/1325-0933$01.50/0

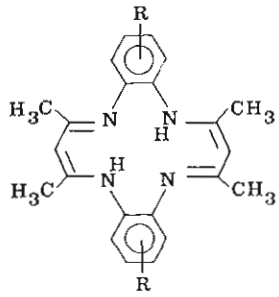

Figure 1. $[H_2Me_4(RBzo)_2[14]tetraeneN_4]$.

XPS measurements were made with a DuPont Model 605B electron spectrometer. Samples were prepared by electropolymerization onto a Pt disk electrode. The Teflon shroud was removed prior to the measurement. Atomic absorption measurements were obtained with an Instruments Laboratory 351 atomic absorption spectrophotometer.

Electrochemical properties were determined in acetonitrile with a 0.1 M tetraalkylammonium salt as supporting electrolyte in conventional three-compartment "H" cells. Cyclic voltammograms were obtained without IR compensation by using a Princeton Applied Research Model 173 potentiostat and a Princeton Applied Research Model 175 programmer and were recorded on a Houston Omnigraph Model 200 X-Y recorder. Electrodes were SnO_2 plates and either platinum or glassy-carbon disks with Teflon shrouds. Electrochemical potentials were recorded vs. a saturated sodium calomel electrode. Before use, the disk electrodes were polished sequentially with 3, 1, and 0.25 μm diamond paste (Buehler) on a Buehler/Ltd apparatus followed by ultrasonic cleaning with a Bronson B-24-4 unit in reagent grade acetonitrile. When necessary, solutions were degassed for approximately 20 min with solvent-saturated Ar.

Apparent surface coverage was calculated as reported by Murray et al.[18] using the equation $\Gamma_{app} = Q_c/(nFA)$ (where Q_c is the charge (area) under the oxidation waves as determined by planimetry, n is the number of electrons per molecule oxidized, F is Faraday's constant and A is the area of the electrode in cm^2). The apparent number of film "layers" was calculated by assuming that a monolayer of material corresponds to 2.43 $\times$ 10^{-11} mol/cm^2, a figure that was calculated on the basis of the dimensions of the R = H complex.[19,20]

Results

Film Growth and Electrochemical Behavior. Oxidation of $Ni[Me_4(RBzo)_2[14]tetraeneN_4]$ (R = CH_3, H, Cl, CO_2CH_3, $CO_2C_3H_7$, NO_2) yields stable, electrochemically active films on electrode surfaces. The films form on Au, Pt, glassy-carbon and SnO_2 surfaces, and they form in solutions of acetonitrile, methylene chloride, or propylene carbonate as solvent with tetraethylammonium perchlorate, tetrabutylammonium perchlorate, tetrabutylammonium hexafluorophosphate, tetraethylammonium hexafluorophosphate or tetraethylammonium *p*-toluenesulfonate as the electrolyte (0.10 M), and one of the nickel derivatives ((0.5–1.0) $\times$ 10^{-3} M) as the electroactive species. The films deposit on the surface by repeatedly scanning the potential region from 0.0 to 1.4 V or from +1.4 to −1.9 V or, alternatively, by holding the potential at 1.4 V vs. SSCE.

Film growth effected by the scanning procedure is illustrated in Figure 2. As shown in Figure 2a, the two oxidation processes previously assigned as ligand-centered[15] become reversible and two commonly observed processes often referred to as prewaves[21] appear at 0.04 and −1.41 V as the film deposits on the electrode surface. The reduction process at −1.73 V remains reversible, but the reduction component of the wave gradually becomes engulfed in the prewave as it forms. As shown in Figure 2b, only the second oxidation wave is observed to grow as the film deposits when the positive region is scanned from 0.0 to 1.4 V. The first oxidation wave centered at 0.45 V is irreversibly coupled with a reduction wave at approximately −1.0 V (Figure 2a) and, consequently, is not observed after the first scan. Film growth by either scanning procedure continued for a large number of scans, but eventually, the current ceased to increase. At this point the film began to passivate with additional scans. Film growth by $Ni[Me_4(RBzo)_2[14]tetraeneN_4]$ (R = CH_3, H, Cl) follows the general patterns illustrated in Figure 2a,b. However, films of the ester (R = CO_2CH_3 and $CO_2C_3H_7$) and NO_2 derivatives remained electrochemically irreversible in the positive region as the film grew on the electrode surface (Figure 2c).

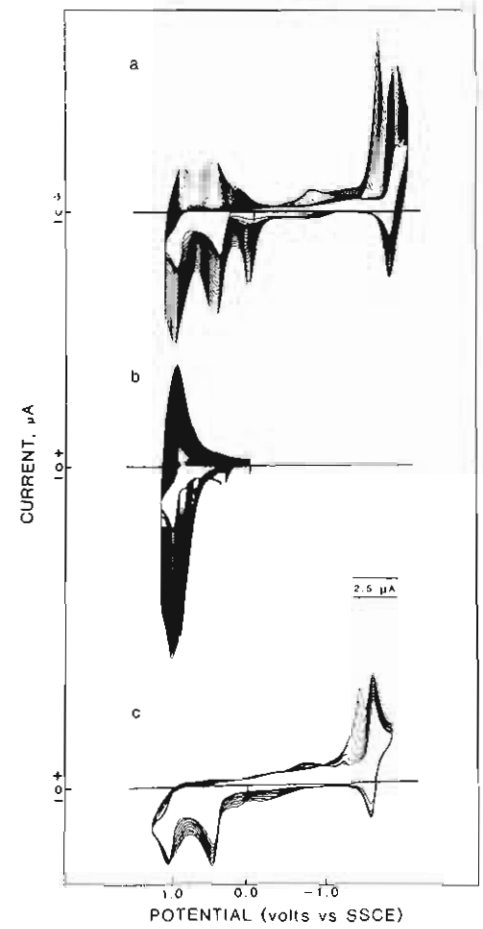

Figure 2. Cyclic voltammograms of film growth on Pt electrodes in acetonitrile solutions containing 0.1 M TEAP and 1.0 $\times$ 10^{-3} M complex: (a) $[Ni(Me_4Bzo_2[14]tetraeneN_4)]$, scan range +1.4 to −1.9 V vs. SSCE; (b) $[Ni(Me_4Bzo_2[14]tetraeneN_4)]$, scan range 0 to 1.4 V vs. SSCE; (c) $[Ni(Me_4(CH_3CO_2Bzo)_2[14]tetraeneN_4)]$, scan range +1.4 to −1.9 V vs. SSCE. The scan rate was 200 mV/s.

Cyclic voltammograms of the surface-modified electrodes in neat electrolyte solution are illustrated in Figure 3. Several differences for the various entries can be noted. In Figure 3a the scan was initiated at 0 V in the negative direction. Surface waves, including prewaves, associated with electrochemical behavior found in solutions are observed. After the positive region was scanned once, the prewave in the negative region increases in magnitude, obscuring the electrochemistry associated with the Ni(II/I) couple (Figure 3b). With thick films (formed with more than 20 scans) one can cycle between the prewaves as shown in Figure 3c, but for thin films (formed with less than ten scans) the prewave in the positive region apparently is embedded under the oxidation waves. As shown in Figure 3d, the surface waves in the positive region for films grown by constant-potential electrolysis contained diffusional characteristics, which disappeared upon scanning the +1.4- to −2.0-V region, and became similar to those obtained by other growth techniques.

The stability of the films was examined by scanning the derivatized electrode in fresh electrolyte and calculating the decrease in charge (area) encompassed by the voltammetric waves. The films formed from the R = H and R = Cl derivatives are relatively

(18) Ellis, C. D.; Margerum, L. D.; Murray, R. W.; Meyer, T. J. *Inorg. Chem.* **1983**, *22*, 1283.
(19) Weiss, M. C.; Gordon, G.; Goedkin, V. L. *Inorg. Chem.* **1977**, *16*, 305.
(20) Hanic, F.; Handlovic, M.; Lindgren, O. *Collect. Czech. Chem. Commun.* **1972**, *37*, 2119.
(21) (a) Abruna, H. D. Ph.D. Dissertation, The University of North Carolina, Chapel Hill, NC, 1980. (b) Ellis, C. D.; Murphy, W. R.; Meyer, T. J. *J. Am. Chem. Soc.* **1981**, *103*, 7480.

Table I. Solution and Surface Redox Properties of $Ni[Me_4(RBzo)_2[14]tetraeneN_4]$ Complexes[a]

	first oxidn			second oxidn			redn		
	surface wave, V		soln wave,[b] V	surface wave, V		soln wave,[b] V	surface wave, V		soln wave,[b] V
R	oxidn	redn	E_{p_1}	oxidn	redn	E_{p_2}	oxidn	redn	$E_{1/2}$
H	0.51	0.51	0.45	0.92	0.92	1.00	−1.81	−1.84	−1.73
CH_3	0.47	0.46	0.39	0.93	0.89	0.97	−1.81	−1.88	−1.79
Cl	0.66	0.67	0.54	1.09	1.06	1.13	−1.63	−1.68	−1.63
CO_2CH_3	0.67		0.59	1.06		1.19	−1.54	−1.56	−1.51
NO_2	0.70		0.82	1.12		1.34	−1.33	−1.25	−1.29

[a] 0.1 M TEAP–acetonitrile solutions; $T = 22 \pm 2$ °C; measured vs. SSCE ± 0.01 V; sweep rates = 200 mV/s. [b] Reference 15.

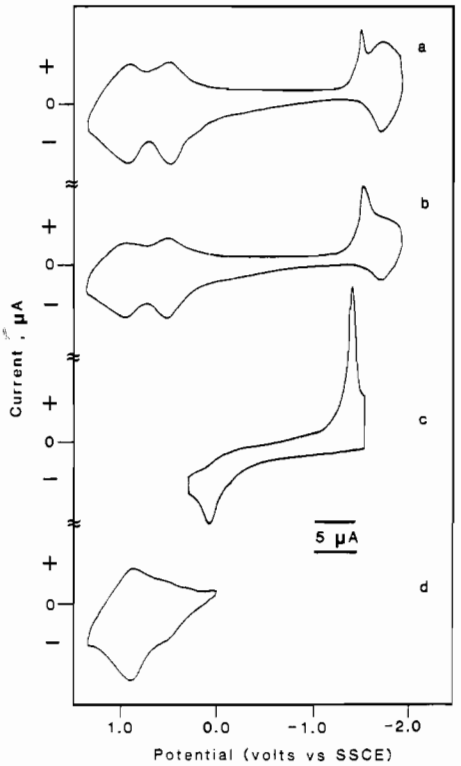

Figure 3. Cyclic voltammograms of $[Ni(Me_4Bzo_2[14]tetraeneN_4)]_n$ films on Pt disk electrodes in acetonitrile solutions containing 0.1 M TEAP: (a) first scan, initiated at 0 V in the negative direction; (b) second scan, continuation of first scan; (c) cycle between prewaves; (d) scan of film deposited by electrolysis at +1.4 V vs. SSCE initiated at 0 V in the positive direction. The scan rate was 200 mV/s.

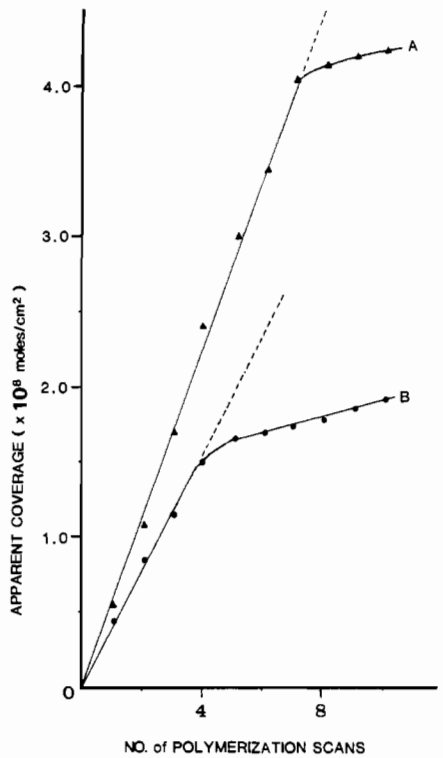

Figure 4. Electrode surface coverage dependence of $[Ni(Me_4Bzo_2[14]-tetraeneN_4)]_n$ on the number of cyclic voltammetric scans: method a, scan range from +1.4 to −2.0 V vs. SSCE; method B, scan range from 0 to 1.4 V vs. SSCE. The solvent was acetonitrile, the electrolyte was 0.1 M TEAP, the complex concentration was 1.0×10^{-3} M, and the scan rate was 200 mV/s.

stable compared to the films containing the R = CH_3 and R = CO_2CH_3 derivatives. Following initial scans in fresh electrolyte, an 11–13% loss of electroactivity was observed for the R = H and R = Cl films for scans from +1.4 to −2.0 V vs. SCCE. The films retained some activity up to approximately 30 scans, after which time only a base line current was observed if cycling was continued. Both the R = CH_3 and the R = CO_2CH_3 films were less stable, with approximately a 30–34% loss of electroactivity occuring after initial scans in fresh electrolyte. The films exhibited no electroactivity following 10–15 scans. However, all derivatized electrodes retained their gold luster for thin films and green color for thicker films following extensive cycling through the electroactive region. This could indicate the film forms an "insulating" layer next to the electrode, which prevents the observation of electroactivity from the outer layers of the film.[18]

In contrast to these results, scans in the negative region from 0 to −2.0 V vs. SSCE resulted in little loss of activity for the films. About 98% activity was retained after 100 scans.

The data obtained for surface and solution potentials are given in Table I. In the positive region, the surface waves moved about 100 mV toward one another with respect to their position in solution. The surface waves in the negative region are approximately in the same location as in solution, but the position of the surface wave associated with the Ni(II) → Ni(I) reduction is shifted somewhat from the true surface value due to the presence and magnitude of the prewave. The surface character of the ester derivatives are less well-defined due to their irreversible character. The position of the waves for analogous processes follow the same substituent trend as in solution, namely $NO_2 > CO_2R > Cl > H > CH_3$.[15]

The apparent surface coverage (determined by integrating the area under the waves in the positive region (0 to 1.4 V) and dividing by the monolayer coverage (2.43×10^{-11} mol/cm^2)) for the nickel macrocycle (R = H) in acetonitrile containing 0.1 M TEAP was determined for various growth techniques. Method *A* involved scanning from +1.4 to −2.0 V during the film growth process, and in method B the scan range was changed to 0.0 to 1.4 V. As shown in Figure 4, the coverage increased at dissimilar rates, with method A yielding a linear increase up to seven scans and method B exhibiting a linear increase up to four scans. For additional scans the apparent surface coverage continued to increase, but at substantially lower rates.

A series of film growth variations for five scans was studied, and the results are tabulated in Table II. The coverage depended on the macrocycle undergoing deposition, the scan rate, the solvent, the electrolyte, and the type of electrode. The nickel macrocycle with R = H gave about three times the coverage as that of R = Cl, which gave about twice the coverage as those with R = CH_3 or R = CO_2CH_3 as the substituent. Since the R = H derivative gave the best coverage, it was used for other comparative growth

Table II. Electrode Surface Coverage by $Ni[Me_4(RBzo)_2[14]tetraeneN_4]$ Complexes[a]

compd	variation	Γ_{app},[b] mol/cm^2	"monolayers"
NiL_{CH_3}	none	5.61×10^{-9}	23
$NiL_{CO_2CH_3}$	none	6.48×10^{-9}	27
NiL_{Cl}	none	1.05×10^{-8}	43
NiL_{H}	none	3.00×10^{-8}	124
	growth range 0.0 to +1.4 V	1.66×10^{-8}	69
	scan rate 50 mV/s	4.51×10^{-8}	185
	glassy-carbon electrode	1.94×10^{-8}	80
	propylene carbonate solvent	2.82×10^{-9}	12
	0.1 M TBAH electrolyte	7.83×10^{-9}	43

[a] Unless otherwise noted, cyclic voltammograms were obtained by using 1×10^{-3} M solutions in 0.1 M TEAP–acetonitrile on a Pt electrode vs. SSCE, scan rate = 200 mV/s, X = 200 mV/cm, and Y = 5 μA/cm. Film growth scan range was from +1.4 to −2.0 V. [b] Area used for apparent surface coverage calculations was from 0.2 to 1.4 V.

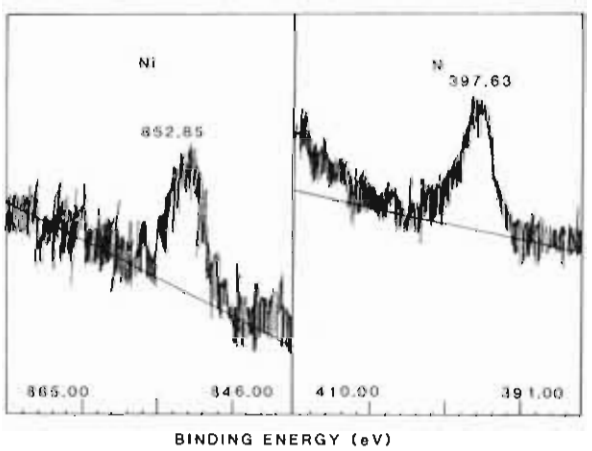

Figure 5. X-ray photoelectron spectra of the $[Ni(Me_4Bzo_2[14]tetraeneN_4)]_n$ film on a Pt support. The film was grown on a Pt disk electrode from an acetonitrile solution that contained 1.0×10^{-3} M complex and 0.1 M TEAP as supporting electrolyte. The scan speed was 200 mV/s, the range was from 1.4 to −2.0 V vs. SSCE, and the number of scans was 25. The normalized intensity of Ni was 0.163; for N it was 0.613.

studies. When the scan range was limited to the oxidation region (i.e. 0.0 to 1.4 V), the surface coverage decreased to approximately one-half the value observed when both the oxidation and reduction region were scanned. The surface coverage at slower scan speeds increased as expected.[22] Films grew more rapidly in acetonitrile than in propylene carbonate. Electrolyte changes from TEAP to TBAH or electrode changes from Pt to glassy-carbon resulted in decreases in the apparent surface coverage.

Characterization of Films Formed from the Nickel Macrocycle (R = H). Constant-potential electrolysis at 1.4 V vs. SSCE yielded a film on a Pt flag electrode and a precipitate in the solution. The precipitate was collected, dissolved in DMF, and identified as $[Ni(Me_4Bzo_2[14]tetraeneN_4)]_2(ClO_4)_2$, on the basis of properties previously reported by Dabrowiak.[16] The material on the electrode surface was mechanically dislodged and found to be insoluble in common solvents, but it could be digested in a mixture of concentrated nitric and sulfuric acids. Solutions of the film prepared in this way were analyzed for their nickel content by atomic absorption spectroscopy. The 11.6% nickel content was consistent with approximately one perchlorate ion incorporated into the film per molecule of nickel macrocycle that deposited. X-ray photoelectron spectra of the film surface on a Pt disk electrode (Figure 5) also confirmed the presence of Ni and gave a Ni to N ratio of 1:4, suggesting that nickel remains coordinated to the macrocycle in the film.

To gain additional understanding of the film's properties, a comparison of its visible–UV and IR spectra to those of the

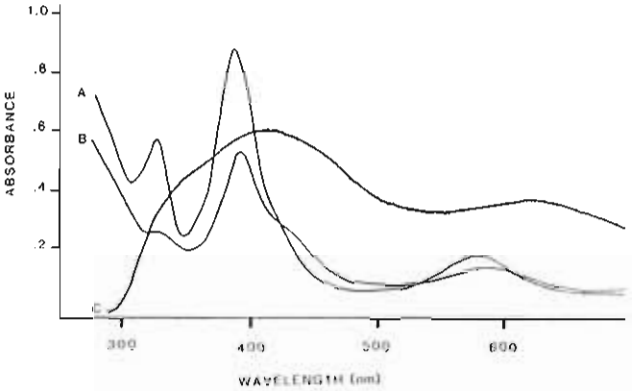

Figure 6. Visible spectra of the monomer, dimer, and polymer derived from $[Ni(Me_4Bzo_2[14]tetraeneN_4)]$: (A) absorption spectrum, 3×10^{-5} M $[Ni(Me_4Bzo_2[14]tetraeneN_4)]$ in DMF; (B) 2×10^{-5} M $[Ni(Me_4Bzo_2[14]tetraeneN_4)]_2(ClO_4)_2$ in DMF; (C) transmission spectrum, $[Ni(Me_4Bzo_2[14]tetraeneN_4)]_n$ on a SnO_2 plate. The absorbance scale for the latter spectrum is arbitrary.

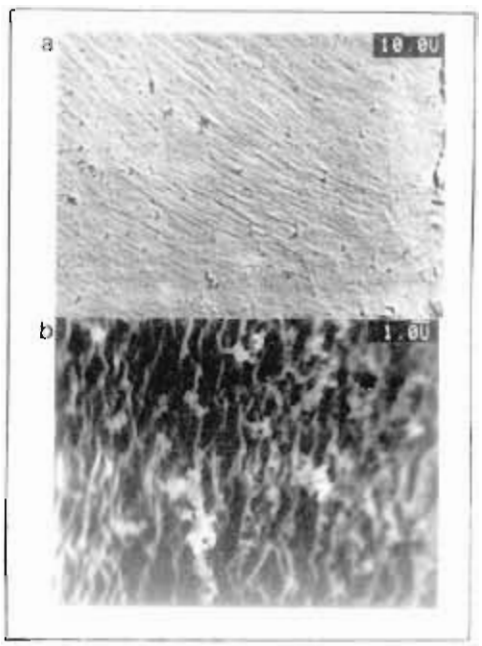

Figure 7. Surface morphology of the $[Ni(Me_4Bzo_2[14]tetraeneN_4)]_n$ film obtained on a Pt surface: (a) lower magnification as indicated; (b) higher magnification as indicated.

monomer $[Ni(Me_4Bzo_2[14]tetraeneN_4)]$ and the dimer $[Ni(Me_4Bzo_2[14]tetraeneN_4)]_2(ClO_4)_2$ were made. Figure 6 shows a comparison of the visible–UV spectra of these compounds in DMF to the film on SnO_2. The lowest energy transition of the monomer at 585 nm is red-shifted upon dimer formation to 595 nm. The peak is further red-shifted in the film to 610 nm. The absorption maximum of the transition of $[Ni(Me_4Bzo_2[14]tetraeneN_4)]$ in a Nujol mull was at 605 nm. Clearly the absorption maximum shift is systematic in going from monomer to dimer and to polymer.

The infrared spectra of the monomer and dimer were obtained by normal dispersive techniques; the film spectrum was obtained by FT-IR spectroscopy. Both the dimer and the film have bands at 630 and 1120 cm^{-1}, which are indicative of ClO_4^- anion. All three exhibit a band at 750 cm^{-1} assigned to ortho-substituted benzene and strong peaks at 1360 cm^{-1} indicative of C—CH_3 vibrations, and some evidence exists for a (>C=N) imine stretch at approximately 1600 cm^{-1}. This latter peak is not well-defined.

Surface Morphology of the Film. Figure 7 contains photographs of the film's surface obtained with a scanning electron microscope. As shown in Figure 7a, the distinct pattern is observed, which is represented by the parallel nature of the film surface. Increasing the magnification (Figure 7b) shows that the surface of the film

(22) Denisevich, P.; Abruna, H. D.; Leidner, C. R.; Meyer, T. J.; Murray, R. W. *Inorg. Chem.* **1982**, *21*, 2153.

Scheme I

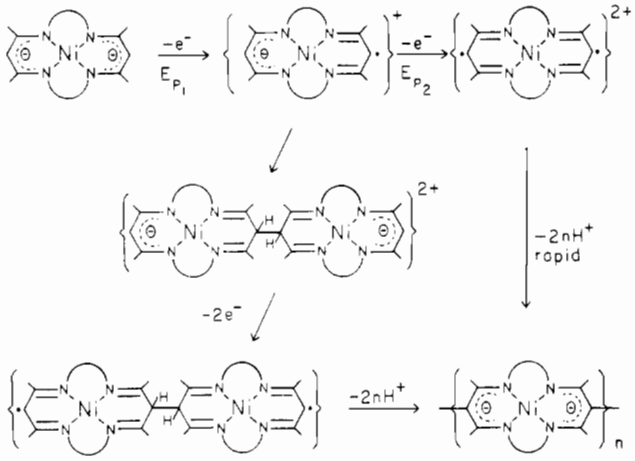

is not smooth; there are holes, and the surface has a ridged appearance. To try to gain additional information about the stacking of layers and thickness of the film, a portion was peeled back and examined with increased magnification. However, not enough contrast existed to obtain meaningful photographs by this technique.

Discussion

Mechanism of Film Growth. The accumulated evidence indicates that the film which results from the oxidation of [Ni(Me_4Bzo_2[14]tetraeneN_4)] is a polymer containing the modified nickel macrocycle. XPS data indicate that the film contains the correct nickel to nitrogen ratio, the visible absorption spectrum is similar to those of [Ni(Me_4Bzo_2[14]tetraeneN_4)] and [Ni(Me_4Bzo_2[14]tetraeneN_4)]$_2(ClO_4)_2$, and the infrared spectra of these compounds are similar. The fact that the visible absorption maximum is red-shifted from 585 nm for the monomer to 610 nm for the compound in the film can be explained by the degree of π delocalization in the ligand framework.[23] The π delocalization over the polymer is greater than that over the dimer; therefore, the visible absorption maximum is shifted further to the red.

The proposed mechanism for film formation is given in Scheme I. Electrode film formation is effected by the technique of electrochemical oxidation.[24] Consequently, the two irreversible oxidations, E_{p_1} and E_{p_2}, are key steps in the mechanism. Removal of electrons at E_{p_1} results in formation of π-cation radicals, which couple to form dimers. The rate at which this occurs appears to be "intermediate" on the cyclic time scale since the reduction component of the E_{p_1} wave can be observed near −1.0 V at scanning rates >50 mV/s. The large potential shift probably results from a rapid structure rearrangement prior to dimer formation. Removal of electrons at E_{p_2} results in formation of π-dication diradicals, which rapidly couple to form a polymer deposit on the electrode surface. This appears to be the predominate polymerization pathway since the redox processes remain the same, implying that an EC mechanism is applicable for formation of the polymer on the electrode surface.

Scheme I is consistent with the experimental facts. Little or no film growth was noted when only the negative voltage region was scanned, while slow film growth occurred when scanning was performed within the +0.7 to −2.0 V range. However, when scanning is extended through the second oxidation wave (i.e. 1.4 V), rapid film growth associated with polymer formation occurs. Scheme I indicates that a pathway to film formation may exist via the dimer, although this reaction is probably slower due to formation of the intervening binuclear radical dication complex. Formation of the dimer by constant-potential electrolysis at 1.4 V can also be explained by the proposed mechanism. Experimentally, the dimer forms at the electrode surface after an initial layer of film was deposited. As the film plates out, a high concentration of protons accumulate near the electrode surface, shifting the equilibrium in favor of protonated dimers, which precipitate due to their insolubility. Also, continuing work in our laboratories indicates that metallotetraazaannulenes that display reversible electrochemistry in the positive voltage region are resistant to film formation on the electrode, verifying the need of short-lived π-cation radicals for polymer film formation.

Properties of the Film. The coupling and deprotonation of radicals in Scheme I results in formation of a polymer that consists of interconnected monomers. The resultant film is unchanged, but according to AA and XPS data, it contains electrolyte. This is not surprising since electrolyte must enter and leave the film during the cycling process. The possibility that the film remained protonated was tested by allowing the film to equilibrate in a 5 mM aqueous ferricyanide solution for 30 min and examining it for ferricyanide incorporation.[25] The resultant cyclic voltammogram in neat electrolyte solution showed only waves due to the film; the ferri/ferrocyanide wave was absent. Addition of pyridine to neat electrolytic solutions or to solutions in which the film was grown passivates the modified electrode. Apparently the amine interacts with nickel's vacant coordination sites, causing the molecules in the film to lose the flexibility needed to remain electrochemically active.[26]

The response of the modified electrodes to other electrochemically active species was examined. Both [Cu(DIM)]$(ClO_4)_2$ (DIM is 2,3-dimethyl-1,4,8,11-tetraazacyclotetradeca-1,3-diene) and *o*-dinitrobenzene normally show reversible electrochemical behavior that falls within the window of the surface-modified electrode. (The potential for $Cu(DIM)^{2+/+}$ is −0.62 vs. SSCE,[27] the first reduction of *o*-dinitrobenzene is at −0.82 V and the second reduction is at −1.09 V vs. SSCE.) In both cases the compounds were reduced at the expected $E_{1/2}$ values, but were not reoxidized until the film first underwent reoxidation. The behavior was similar, in some respects, to that found for bilayer electrodes.[28]

The behavior of prewaves for thick films resembled that of previously published systems.[18,22,28c] The cathodic prewave grows at the foot of the nickel(II) reduction wave; the anodic prewave grows at the foot of the ligand oxidation wave. The behavior of the cathodic prewave is more easily tracked. It begins forming away from the main wave and gradually moves toward it, increasing in magnitude with the number of scans, and eventually becomes dominant. The anodic prewave exhibits two types of behavior. It grows at the foot of the first oxidation wave for thick films when scanning is performed from +1.4 to −2.0 V vs. SSCE but also grows at the foot of the second oxidation wave when the first is absent (0 to 1.4 V). In neat electrolyte, the anodic prewave for thin film lies under the two oxidation waves in the positive voltage region. Regardless of film thickness, the prewaves behave as redox-coupled pairs; reversing the scan prior to passing through its complement greatly diminishes the magnitude of its current. In this respect, the prewaves resemble the effects attributed to bilayer electrodes.[28]

The surface redox potentials of the R = H, Cl, and CH_3 derivatives follow normal surface behavior, with the oxidation and reduction waves of a given redox process lying at nearly the same potentials and are readily assigned by comparison to the processes that occur in solution. $E_0'(1)$ corresponds to the removal of the first π electron from the ligand as shown in eq 1; $E_0'(2)$ corresponds to removal of the second electron as shown in eq 2; $E_0'(3)$ corresponds to the Ni(II/I) couple as depicted in eq 3. The ligand

(23) Rillema, D. P.; Mack, K. B. *Inorg. Chem.* **1982**, *21*, 3849.
(24) Merz, A.; Bard, A. J. *J. Am. Chem. Soc.* **1978**, *100*, 3222.
(25) Oyama, N.; Ohsaka, T.; Kaneko, M.; Sato, K.; Matsuda, H. *J. Am. Chem. Soc.* **1983**, *105*, 6008.
(26) (a) Moses, P. R.; Murray, R. W. *J. Am. Chem. Soc.* **1976**, *98*, 7435. (b) Moses, P. R.; Wier, L. M.; Lennox, J. C.; Finklea, H. D.; Lenhard, J. R.f Murray, R. W. *Anal. Chem.* **1978**, *50*, 576.
(27) Fabbrizzi, L.; Lari, A.; Poggi, A.; Seghi, B. *Inorg. Chem.* **1982**, *21*, 2083.
(28) (a) Abruna, H. D.; Denisevich, P.; Umana, M.; Meyer, T. J.; Murray, R. W. *J. Am. Chem. Soc.* **1981**, *103*, 1. (b) Denisevich, P.; Willman, K.; Murray, R. W. *J. Am. Chem. Soc.* **1981**, *103*, 4127. (c) Ellis, C. D.; Murphy, W. R.; Meyer, T. J. *J. Am. Chem. Soc.* **1981**, *103*, 7480. (d) Murao, K.; Suzuki, K. *J. Chem. Soc., Chem. Commun.* **1984**, 238.

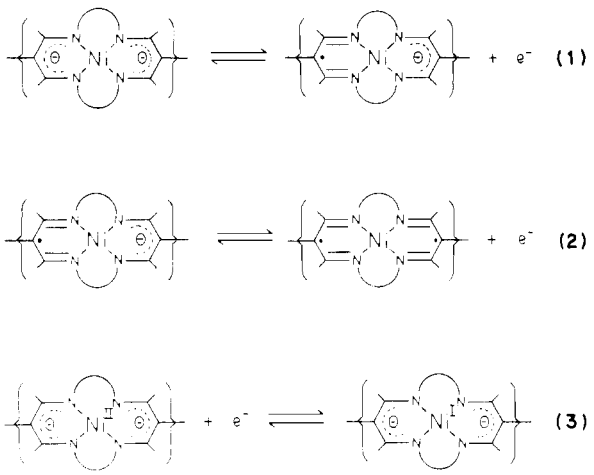

oxidation waves that were irreversible in solution now are reversible. The Ni(II/I) couple would also demonstrate reversible surface behavior, were it not for the presence of the prewave.

Conclusion. The electropolymerization of nickel tetraazaannulenes on electrode surfaces is a unique method to add to electropolymerization techniques currently used to modify electrode surfaces.[29] These tetraazaannulene, surface-modified electrodes are important from a number of viewpoints. Thin, homogeneous films can be deposited on the electrode surface, and the surface potentials can be controlled by varying the substituents on the ligand, the metal center, and/or the ligands themselves. Since the polymerization is ligand-centered, it should be possible to prepare copolymer films coupling the appropriate tetraazaannulenes that conduct over a large potential region. It should also be possible to design rectifiers and diodes by the sequential polymerization of the appropriate tetraazaannulenes on the electrode surface. These surface-modified electrodes should then find use in catalysis and fuel cells and could serve as electronic devices. We currently are extending our studies into these areas and plan to report our results in the near future.

Acknowledgment. This work was supported by the Office of Naval Research and the North Carolina Biotechnology Center. D.P.R. thanks the American Society of Engineering Education for a 1983 Summer Faculty Fellowship with the Department of the Navy. Thanks also are given to Sador S. Black at N. C. State for the AA analyses, Steve Simko at UNC-Chapel Hill for the XPS film analyses, and Eddie Stokes at UNCC for the SEM work. This is paper No. 7 from the North Carolina Biomolecular Engineering and Materials Application Center.

Registry No. $Ni[Me_4Bzo_2[14]tetraeneN_4]$, 51223-51-9; $Ni[Me_4(CH_3Bzo)_2[14]tetraeneN_4]$, 74834-16-5; $Ni[Me_4(ClBzo)_2[14]tetraeneN_4]$, 92396-74-2; $Ni[Me_4(CO_2CH_3Bzo)_2[14]tetraeneN_4]$, 92396-70-8; $Ni[Me_4(NO_2Bzo)_2[14]tetraeneN_4]$, 92396-72-0; $Ni[Me_4(CO_2C_3H_7Bzo)_2[14]tetraeneN_4]$, 92396-71-9; $[Ni(Me_4Bzo_2[14]tetraeneN_4)]_2(ClO_4)_2$, 100570-25-0; $[Ni(Me_4(CH_3Bzo)_2[14]tetraeneN_4)]_n$, 100485-73-2; $[Ni(Me_4Bzo_2[14]tetraeneN_4)]_n$, 100485-74-3; $[Ni(Me_4(ClBzo)_2[14]tetraeneN_4)]_n$, 100485-75-4; $[Ni(Me_4(CO_2CH_3Bzo)_2[14]tetraeneN_4)]_n$, 100485-76-5; $[Ni(Me_4(CO_2C_3H_7Bzo)_2[14]tetraeneN_4)]_n$, 100485-77-6; $[Ni(Me_4(NO_2Bzo)_2[14]tetraeneN_4)]_n$, 100485-78-7; $Cu(DIM)^{2+}$, 80502-49-4; $Cu(DIM)^{+}$, 80502-50-7; Bu_4NPF_6, 3109-63-5; Et_4NClO_4, 2567-83-1; SnO_2, 18282-10-5; Pt, 7440-06-4; carbon, 7440-44-0; *o*-dinitrobenzene, 528-29-0.

(29) Murray, R. W. *Annu. Rev. Mater. Sci.* **1984**, *14*, 145 and references therein.

Contribution from the Departments of Chemistry, Texas A&M University, College Station, Texas 77843, and College of General Education, Kyushu University, Fukuoka, Japan

Cascade Halide Binding by Multiprotonated BISTREN and Copper(II) BISTREN Cryptates

Ramunas J. Motekaitis,[†] Arthur E. Martell,*[†] and Ichiro Murase[‡]

Received June 11, 1985

The macrobicyclic ligand 7,19,30-trioxa-1,4,10,13,16,22,27,33-octaazabicyclo[11.11.11]pentatriacontane, BISTREN, has been synthesized in sufficient quantity to carry out a detailed investigation of halide binding to its protonated forms and to its mononuclear and binuclear Cu(II) complexes. Potentiometric investigations were conducted at 1.000 M ionic strength at 25.0 °C in supporting electrolytes consisting of 1.000 M $NaClO_4$ and NaF, 1.000 M NaCl, 1.000 M NaBr, and 1.000 M NaI, in the absence and in the presence of 1 and 2 mole ratios of Cu(II) to ligand. Some combinations of the supporting halide electrolytes with $NaClO_4$ to a total ionic strength of 1.000 M were also employed. A special procedure was required for the system containing Cu(II) and I^-. On the basis of the assumption of no binding to perchlorate, by comparison of the macroscopic protonation and Cu(II) formation constants, in the presence and absence of the halide ions, quantitative calculations of the halide binding constants were carried out. Results are reported for binding by the protonated ligand of HF_2^-, F^-, Cl^-, Br^-, and I^- and for the binding of all four halide ions to the protonated mononuclear Cu(II) cryptate and to the binuclear Cu(II) cryptate.

Introduction

BISTREN is a macrobicyclic ligand that can coordinate one to six protons and/or one or two metal ions in aqueous solution. It consists of two 2,2′,2″-triaminotriethylamine (TREN) moieties tied together with five-atom diethyl ether bridges. Although it contains eight amino groups, the tertiary bridgehead nitrogens are so weakly basic, because of Coulombic repulsion of adjacent protonated nitrogens, that the hexaprotonated form is the most acid species in aqueous solution under the conditions that can be employed for potentiometric measurements. Therefore, BISTREN may be designated an H_6L^{6+} ligand, corresponding to the form generally employed (the hexahydrobromide) for potentiometric investigations.

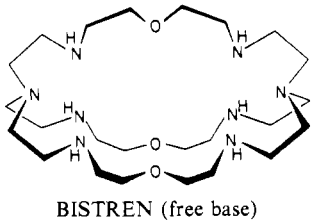

BISTREN (free base)

[†] Texas A&M University.
[‡] Kyushu University.

0020-1669/86/1325-0938$01.50/0